

## SHORT COMMUNICATION

# A hyperpolarizing rod bipolar cell in the sea lamprey, *Petromyzon marinus*

Rikard Frederiksen<sup>1,\*</sup>, Gordon L. Fain<sup>1,2</sup> and Alapakkam P. Sampath<sup>1</sup>

**ABSTRACT**

Retinal bipolar cells receive direct input from rod and cone photoreceptors and send axons into the inner retina, synapsing onto amacrine and ganglion cells. Bipolar cell responses can be either depolarizing (ON) or hyperpolarizing (OFF); in lower vertebrates, bipolar cells receive mixed rod and cone input, whereas in mammals, input is mostly segregated into 14 classes of cone ON and OFF cells and a single rod ON bipolar cell. We show that lamprey, like mammals, have rod bipolar cells with little or no cone input, but these cells are OFF rather than ON. They have a characteristic morphology and a spectral sensitivity nearly indistinguishable from that of rod photoreceptors. In background light known to saturate rods, rod bipolar cells are also saturated and cannot respond to increment flashes. Our results suggest that early vertebrate progenitors of both agnathans and gnathostomes may have had a more fluid retinal organization than previously thought.

**KEY WORDS:** Retina, Rod, Cone, Photoreceptor, ON cells, OFF cells

**INTRODUCTION**

Retinal bipolar cells receive direct input at their dendrites from photoreceptors in the outer plexiform layer (OPL) and send axons into the inner plexiform layer (IPL), where they synapse onto amacrine and ganglion cells. Bipolar cells are of two types (Kaneko, 1970; Werblin and Dowling, 1969): depolarizing or ON bipolar cells, for which photoreceptor input produces an increase in conductance and an inward current during illumination; and hyperpolarizing or OFF cells, for which photoreceptors produce a decrease in conductance and an outward current in the light. In the mouse retina, which has been particularly well characterized, there are 15 kinds of bipolar cells (Shekhar et al., 2016; West and Cepko, 2021). One, called the rod bipolar, is dominated by rod input, and some cells receive input only from rods; however, some can also receive input from cones (Behrens et al., 2016; Pang et al., 2010). Rod bipolar cells in mammals are always ON and provide the major pathway for the flow of rod signals from the outer to the inner retina (Grimes et al., 2018). There are also 14 classes of cone bipolar cells, which can be either ON or OFF. Some OFF cone bipolar cells may also receive direct input

from rods (Behrens et al., 2016; Hack et al., 1999; Li et al., 2004; Soucy et al., 1998).

In lower vertebrates, bipolar cells generally receive both rod and cone input but can be classified as rod dominated or cone dominated, depending on the proportion of photoreceptor synapses or input signal the cells display (Connaughton et al., 2004; Ishida et al., 1980; Scholes, 1975; Wu et al., 2000). Rod-dominated bipolar cells are generally ON (Ashmore and Falk, 1980; Connaughton, 2001; Hensley et al., 1993; Wu et al., 2000) and, like the rod bipolar cells in mammals (Wassle et al., 1991), can be marked with antibodies to protein kinase C (Yazulla and Studholme, 2001). Rod-dominant OFF bipolar cells have, however, been observed in salamander (Hensley et al., 1993; Wu et al., 2000). Cone-dominated bipolar cells (ON or OFF), like those in mammals, can receive input exclusively from cones or can be mixed rod–cone (Connaughton et al., 2004; Fain, 1975; Hensley et al., 1993; Ishida et al., 1980; Wu et al., 2000). There are no reports in lower vertebrates of bipolar cells receiving only rod input. These findings suggest that bipolar cells in all vertebrates evolved largely as rod-dominant ON and cone-dominant ON and OFF, with rod bipolar cells receiving a variable (and usually small) contribution from cones, and cone bipolar cells a similar and usually small input from rods.


Lamprey are cyclostomes and jawless vertebrates (agnathans), whose progenitors diverged from all other vertebrates in the late Cambrian approximately 500 million years ago (Kuraku and Kuratani, 2006). We have previously shown that the lamprey retina has both ON and OFF bipolar cells, and that the ON bipolar responses can be blocked with L-2-amino-4-phosphonobutyrate (APB or L-AP4) and are probably mediated by metabotropic mGluR6 glutamate receptors (Ellis et al., 2020), as in all other vertebrates. In the process of investigating rod and cone input to these cells, we discovered an abundant cell type with cell bodies abutting the photoreceptor synaptic layer and axons penetrating deep into the IPL, reminiscent of the mammalian rod bipolar cell (Dacheux and Raviola, 1986). These cells receive input almost exclusively from rods but are OFF instead of ON, suggesting that the evolution of bipolar cells in vertebrate retina may have been more fluid than previously thought.

**MATERIALS AND METHODS**

This study was carried out in accordance with the recommendations of the Guide for the Care and Use of Laboratory Animals of the National Institutes of Health, USA, and was approved by the University of California Los Angeles Animal Research Committee. Sea lamprey, *Petromyzon marinus* Linnaeus 1758, were provided to us by the Hammond Bay Biological Station of the United States Geological Survey (USGS), Millersburg, MI, USA. They were kept in a large fresh-water aquarium at 4°C on a 12 h:12 h light:dark cycle. All experiments were performed on fully metamorphosed juvenile animals, because of the greater ease of tissue preparation.

<sup>1</sup>Stein Eye Institute, David Geffen School of Medicine, University of California Los Angeles, Los Angeles, CA 90095-7000, USA. <sup>2</sup>Department of Integrative Biology and Physiology, University of California Los Angeles, Los Angeles, CA 90095-7239, USA.

\*Author for correspondence (frederiksen@sei.ucla.edu)

 R.F., 0000-0001-7999-8480; G.L.F., 0000-0002-9813-0342; A.P.S., 0000-0002-0785-9577

## Anatomy

Lamprey eyes were fixed in 2% formaldehyde and 2.5% glutaraldehyde in 0.1 mol l<sup>-1</sup> sodium phosphate buffer (PBS) overnight at 4°C. The tissue was post-fixed with 1% osmium tetroxide in PBS, dehydrated in a graded series of alcohols, and embedded in Epson resin. Semi-thin sections (1 µm) were stained with 0.5% Toluidine Blue in 1% sodium borate. The light micrographs were photographed with a Zeiss Axiophot microscope equipped with a 40× oil immersion objective and a CoolSNAP digital camera.

## Solutions

For dissection and tissue storage, we used oxygenated (100% O<sub>2</sub>) Ames' solution buffered with Hepes (2.38 g l<sup>-1</sup>) at pH 7.4. The osmolarity was measured with a vapor-pressure osmometer (Wescor, Logan, UT, USA) and adjusted to 282–286 mOsm by the addition of NaCl (0.875 g l<sup>-1</sup>). Tissue was stored in this solution in a dark container on ice. For patch-clamp recording, the retinal slice was superfused at a rate of 4 ml min<sup>-1</sup> with Ames' medium buffered with NaHCO<sub>3</sub> (1.9 g l<sup>-1</sup>) and equilibrated with 95% O<sub>2</sub>/5% CO<sub>2</sub> at pH 7.4. The osmolarity of the medium was adjusted to 282–286 mOsm. Temperature was maintained at room temperature (20–25°C) throughout the recording. The internal solution used for recording pipettes contained (in mmol l<sup>-1</sup>): 125 potassium aspartate, 10 KCl, 10 Hepes, 5 NMDG-HEDTA, 0.5 CaCl<sub>2</sub>, 0.5 MgCl<sub>2</sub>, 0.1 ATP-Mg, 0.5 GTP-TRIS and 2.5 NADPH. The pH was adjusted to 7.30±0.02 with NMDG-OH, and the osmolarity was adjusted to 278±1 mOsm. We added to the internal solution a fluorescent dye (100 µmol l<sup>-1</sup>; Alexa Fluor 750, λ<sub>max</sub> ~750 nm; ThermoFisher, Waltham, MA, USA), which diffused into the target cell during recording.

## Patch-clamp recording

We made voltage-clamp recordings from lamprey bipolar cells as in our earlier work (Ellis et al., 2020), using methods previously described (Ingram et al., 2019; Okawa et al., 2010). After overnight dark adaptation, the animal was euthanized and enucleated under near-infrared (NIR) light with the aid of infrared image converters (ITT Industries, White Plains, NY, USA). The anterior portion of the eye was removed, and the retina was isolated free of retinal pigment epithelium in Hepes-buffered Ames' solution. The isolated retinal piece was embedded in 3% low-temperature-gelling agar in Hepes-buffered Ames' solution. In cold Hepes-buffered Ames' solution, 200 µm-thick slices were cut with a vibratome (Leica VT-1000S); the retina was cut vertically to maintain neural circuitry. Cut slices were transferred to dishes, which were placed on the stage of the set-up for immediate recording.

Filamented borosilicate glass capillaries (BF120-69-10; Sutter Instruments, Novato, CA, USA) were pulled the day of the experiment with a P-97 Flaming/Brown micropipette puller (Sutter Instruments). Pipettes had a resistance of 16–18 MΩ. Cells were patch clamped in the whole-cell configuration and recorded in voltage-clamp mode at a clamp potential of -40 mV (rods and cones) or -60 mV (bipolar cells). Series resistance was compensated at ~80%. Cells could be provisionally identified based on their position in the retina, morphology, sensitivity and response waveform.

The recording set-up consisted of a Nikon Eclipse E600N microscope to hold and view the preparation, Sutter Instruments MP285 micro-manipulators, and an Axopatch 200B amplifier (Molecular Devices, San Jose, CA, USA). The microscope was also equipped with a Watec 902HB camera (Pine Bush, NY, USA) for

viewing the preparation under NIR illumination. Images (NIR and fluorescence) were captured with a Nikon Digital SightQiMc camera and Nikon Elements software. Excitation light for fluorescence imaging was provided by a Nikon xenon arc lamp coupled to the epifluorescence port of the microscope via a light guide. For fluorescence imaging, we used a cy7 filter set (Chroma, Bellows Falls, VT, USA).

Stimulus and background light were delivered with a dual OptoLED light source (Cairn Research, Faversham, UK) coupled to a custom-built, dual-pathway optical system for uniform, calibrated illumination of the preparation. One of the light paths had a 405 nm LED that was attenuated by absorptive neutral-density filters. The other light path had a white LED coupled to 10 nm bandwidth interference filters with peak wavelengths at 450, 500, 540, 560, 600 and 620 nm, attenuated by absorptive neutral-density filters. Interference filters and neutral-density filters were changed by computer-controlled motorized filter wheels. The two photostimulator beams were combined by means of a dichroic mirror and then further combined with a NIR (840 nm) beam for viewing. All optical components in the photostimulator were purchased from Thorlabs Inc. (Newton, NJ, USA).

The intensity of the stimulus was calibrated with a photodiode (Graseby Optronics, Orlando, FL, USA) connected to a PDA200C amplifier (Thorlabs Inc.). Recordings were low-pass filtered at 70 Hz with a tunable active filter (Frequency Devices Inc., Ottawa, IL, USA) and digitized at 10 kHz with an InstruTech ITC-18 D/A and A/D board (Port Washington, NY, USA). Data were collected with a MATLAB-based acquisition package (MathWorks, Natick, MA, USA) and the Symphony Data Acquisition System (<https://open-ephys.org/symphony/>).

## Data analysis

Images were processed with ImageJ open-source software. Fluorescent images were pseudo-colored and merged with the wide-field images captured under NIR illumination to determine the location and morphology of the recorded cell.

Recorded traces were baseline subtracted, averaged, and sampled at 1 kHz with the Iris DVA custom MATLAB data analysis package (open source: <https://github.com/sam-path-lab-ucla/IrisDVA>). Data analysis, curve fitting and plotting were done in Python. Amplitudes of recorded photocurrents were derived and plotted against flash intensity of the stimulus light in photoisomerizations ( $R^*$  or  $P^*$ ) per photoreceptor. They were fitted with the Michaelis–Menten equation:

$$R = \frac{(R_{\max}\phi)}{(\phi + \phi_{1/2})}, \quad (1)$$

where  $R$  is the response amplitude (photocurrent),  $R_{\max}$  is the saturated response amplitude,  $\phi$  is flash intensity, and  $\phi_{1/2}$  is the value of  $\phi$  that evokes a half-maximal response.

The number of photoisomerizations ( $R^*/\text{rod}$  or  $P^*/\text{cone}$ ) caused by a flash was calculated by multiplying the flash intensity by the collecting area and adjusting for the stimulus wavelength in relation to the absorbance spectrum of the visual pigment. We used a collecting area of 0.35 µm<sup>2</sup> for rods (Morshedean and Fain, 2017). For cones, we adjusted for their smaller outer segment volume (a factor of 0.4 compared with rods; see Dickson and Graves, 1979; Hárosi and Kleinschmidt, 1993; Morshedean and Fain, 2017) and estimated a collecting area of 0.14 µm<sup>2</sup>.

Spectral sensitivity was derived by measuring sensitivity at each of the tested wavelengths, calculated as the photocurrent

evoked by a light stimulus within the linear range of the response–intensity relationship ( $<10\%$  of  $R_{\max}$ ), divided by the stimulus intensity. These values were then plotted against the wavelength of the stimulus and fitted with a rhodopsin A1 nomogram (Govardovskii et al., 2000). Data are presented as means  $\pm$  s.e.m., with the sample size  $n$  giving the number of recorded cells.

## RESULTS AND DISCUSSION

In a previous publication, we showed that the sea lamprey retina has both ON and OFF bipolar cells (Ellis et al., 2020). The cells we recorded in this earlier study were usually found in the middle of the inner nuclear layer (INL) and appeared to have both rod and cone input. As we continued to record from lamprey retina, we encountered an abundant cell type situated in the outer part of the INL in close proximity to the OPL, which was particularly easy to

visualize in juvenile animals (Fig. 1A). Because these cells bear a superficial resemblance to rod bipolar cells in mammals (e.g. Dacheux and Raviola, 1986), we singled them out for further investigation.

Fig. 1A shows a light micrograph of a transverse section through a sea lamprey retina taken close to the optic nerve head. We have indicated members of the relevant population of bipolar cells with arrowheads. Cells like these were targeted in patch-clamp recording from retinal slices, were filled with Alexa 750 fluorescent dye, and were imaged (Fig. 1B). The fluorescent images were pseudo-colored and merged with images captured under NIR illumination to produce a composite image, where the filled cell appears in red (Fig. 1C). These cells had dendritic terminations in the OPL as well as a long axon descending into the INL and forming at least two branches (Fig. 1B,C). They also had a process extending into the outer nuclear layer (ONL) resembling a Landolt's club, as for

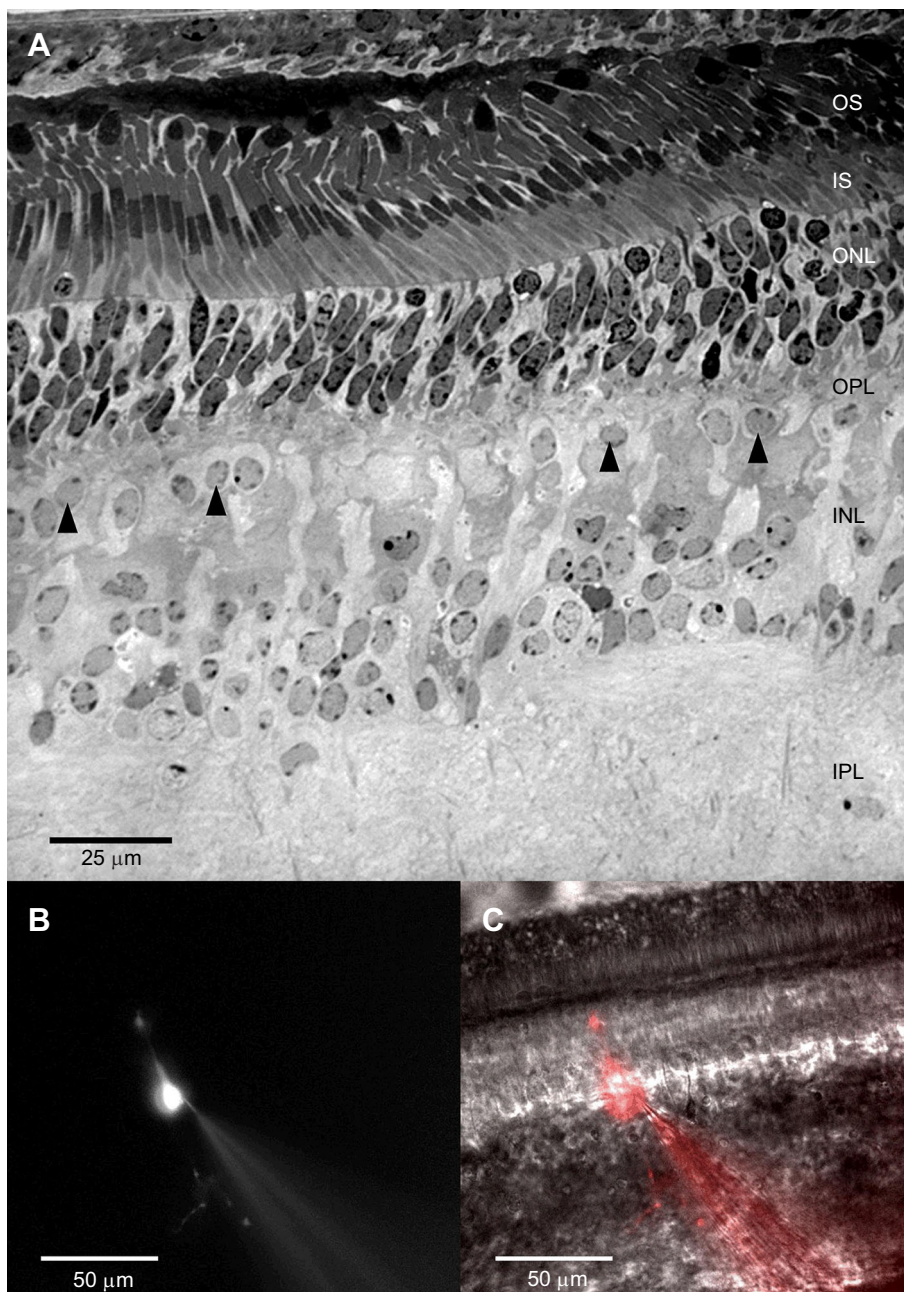


**Fig. 1. Retinal morphology of sea lamprey, *Petromyzon marinus*.** (A) Light micrograph showing a transverse section of the retina of a juvenile lamprey cut close to the optic nerve, with the photoreceptors at the top of the panel. OS, outer segments; IS, inner segments; ONL, outer nuclear layer; OPL, outer plexiform layer; INL, inner nuclear layer; IPL, inner plexiform layer. Arrowheads indicate cell bodies of putative rod OFF bipolar cells. (B) Rod OFF bipolar cell filled with Alexa Fluor 750 dye and imaged with a cy7 filter set. (C) Same cell as in B, overlaid on a wide-field image viewed under near-infrared illumination (840 nm).



bipolar cells of other non-mammalian vertebrates (Hendrickson, 1966; Quesada and Génis-Gálvez, 1985).

### Light responses of bipolar cells

In Fig. 2A–C, we show current responses to a series of flash stimuli from a rod, a cone and a bipolar cell. The bipolar cell, like both the rod and cone, responded to light with an outward (hyperpolarizing) current. Bipolar cell light responses were slow and rod-like, with no clear initial fast component indicating cone input as in our previous study (Ellis et al., 2020).

A more quantitative description of sensitivity is given in Fig. 2D. For all three cell types, we could obtain a good fit of response amplitude as a function of the strength of the stimulus with a Michaelis–Menten function (Eqn 1). The range of responsiveness (from threshold to saturation) spanned about 2 orders of magnitude for all three cell types. The flash sensitivity of the bipolar cell ( $8.8 \pm 2.1 \text{ pA } \phi^{-1} \mu\text{m}^2$ ) from these measurements was about 38 times that of the rod ( $0.24 \pm 0.061 \text{ pA } \phi^{-1} \mu\text{m}^2$ ) and about 1500 times that of the cone ( $0.0057 \pm 0.0011 \text{ pA } \phi^{-1} \mu\text{m}^2$ ). These data seemed to suggest that these OFF bipolar cells receive mainly rod input.

To test this hypothesis, we measured the spectral sensitivity of the OFF bipolar cells and of the photoreceptors. Sea lamprey have only a single kind of rod and a single kind of cone (Morshedian et al., 2017; see also Hárosi and Kleinschmidt, 1993), and juveniles have vitamin A1-based visual pigments with peak sensitivities near 500 nm for rods and 550 nm for cones. We accordingly used A1 nomograms (Govardovskii et al., 2000) to fit our spectral sensitivity measurements. These results are given in Fig. 2E. Both the rod and the OFF bipolar cell sensitivities could be well fitted by an A1 curve with peak at 498 nm, whereas the cone sensitivities could be fitted by a curve with a peak at 555 nm. The difference in sensitivity between rod and rod bipolar cells was smaller in these

experiments (about a factor of 23) than for those of Fig. 2D (about 38); we think this small discrepancy can be attributed to experimental error.

### OFF bipolar cells are saturated in bright light

The sensitivities of the OFF bipolar cells were marginally greater at 600 and 620 nm than our best-fitting nomogram. It is possible that this discrepancy is due to experimental error, but it seemed to us also possible that the OFF bipolar cells received some small input from cones. As a further test for cone input, we recorded response families from the bipolar cells in the presence of a bright background light bleaching 6000 rhodopsin molecules per second ( $R^* \text{ s}^{-1}$ ). This background intensity was chosen because it is bright enough to keep rods in saturation (Morshedian and Fain, 2017) and would effectively block their synaptic input to the bipolar cells. The cones, in contrast, gave robust responses in this background intensity (Morshedian and Fain, 2017). Thus, if cone signals were coming into the bipolar cells, we should be able to record some response in the presence of the background light.

The results of these experiments are presented in Fig. 3A–C and summarized in Fig. 3D. These data show that no detectable response could be recorded from the OFF bipolar cells in the presence of a background light saturating the rods, and that the cells recovered their responsiveness once the background light was turned off. These experiments seem to exclude any significant cone input to the OFF rod bipolar cells. As a control experiment, we repeated the same protocol on an OFF bipolar cell receiving input from both rods and cones. The data in Fig. 3E–G clearly show that this cell was able to respond under the same background light conditions. The marked change in the waveform of the response in the presence of the background light could have been the result of saturation of rod input to horizontal cells, which were providing inhibitory input to the bipolar cell.

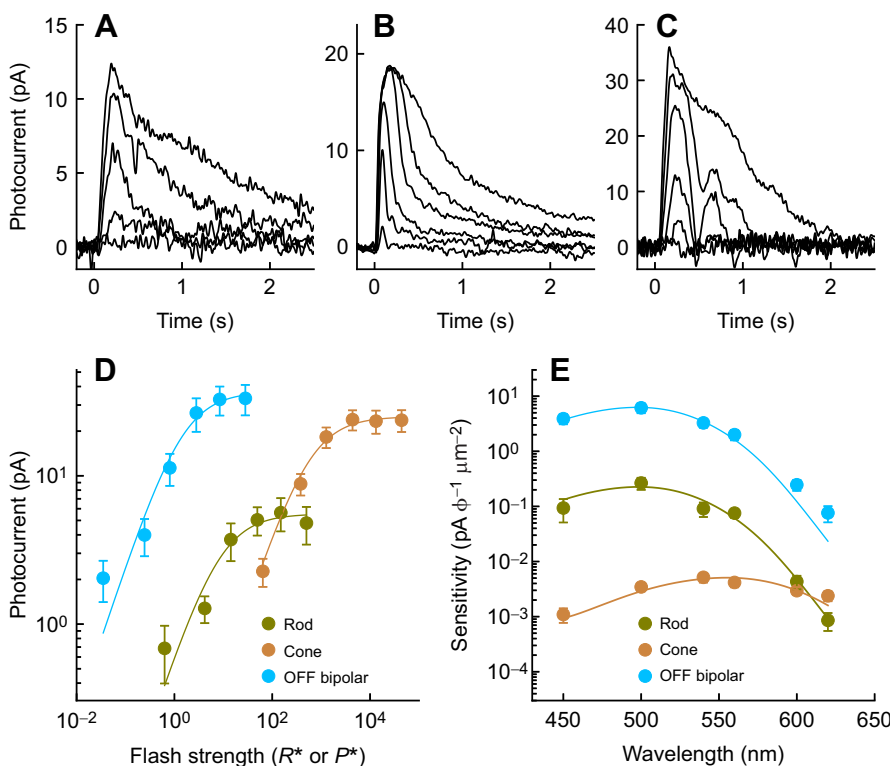


**Fig. 2. Response–intensity relationships and spectral sensitivity of rods, cones and rod OFF bipolar cells.** (A) Family of responses recorded from a rod to 500 nm flash stimuli of 0.6, 4.2, 14, 49 and 150  $R^*/\text{rod}$ . (B) Family of responses recorded from a cone to 540 nm flash stimuli of 64, 370, 1300, 4400, 13,000 and 44,000  $P^*/\text{cone}$ . (C) Family of responses recorded from a rod OFF bipolar cell to 500 nm flash stimuli of 0.035, 0.24, 0.80, 2.8, 8.4 and 28  $R^*/\text{rod}$ . Flashes in A–C were 8 ms. (D) Response–intensity relationships of rods ( $n=5$ ), cones ( $n=6$ ) and OFF bipolar cells ( $n=11$ ). Data were fitted with Eqn 1. Best-fitting parameters were: rods,  $R_{\text{max}}=5.53 \text{ pA}$  and  $\phi_{1/2}=8.42 R^*$ ; cones,  $R_{\text{max}}=25.0 \text{ pA}$  and  $\phi_{1/2}=563 P^*$ ; and OFF bipolar cells,  $R_{\text{max}}=36.9 \text{ pA}$  and  $\phi_{1/2}=1.44 R^*$ . (E) Spectral sensitivity of rods ( $n=12$ ), cones ( $n=12$ ) and OFF bipolar cells ( $n=8$ ). Data were fitted with A1 nomograms (Govardovskii et al., 2000), where the parameters  $S_{\text{peak}}$  and  $\lambda_{\text{max}}$  represent the peak sensitivity and the wavelength at peak sensitivity. Best-fitting parameters were: rods,  $\lambda_{\text{max}}=498 \text{ nm}$  and  $S_{\text{peak}}=0.23 \text{ pA } \phi^{-1} \mu\text{m}^2$ ; cones,  $\lambda_{\text{max}}=555 \text{ nm}$  and  $S_{\text{peak}}=0.0051 \text{ pA } \phi^{-1} \mu\text{m}^2$ ; and OFF bipolar cells,  $\lambda_{\text{max}}=498 \text{ nm}$  and  $S_{\text{peak}}=6.3 \text{ pA } \phi^{-1} \mu\text{m}^2$ .

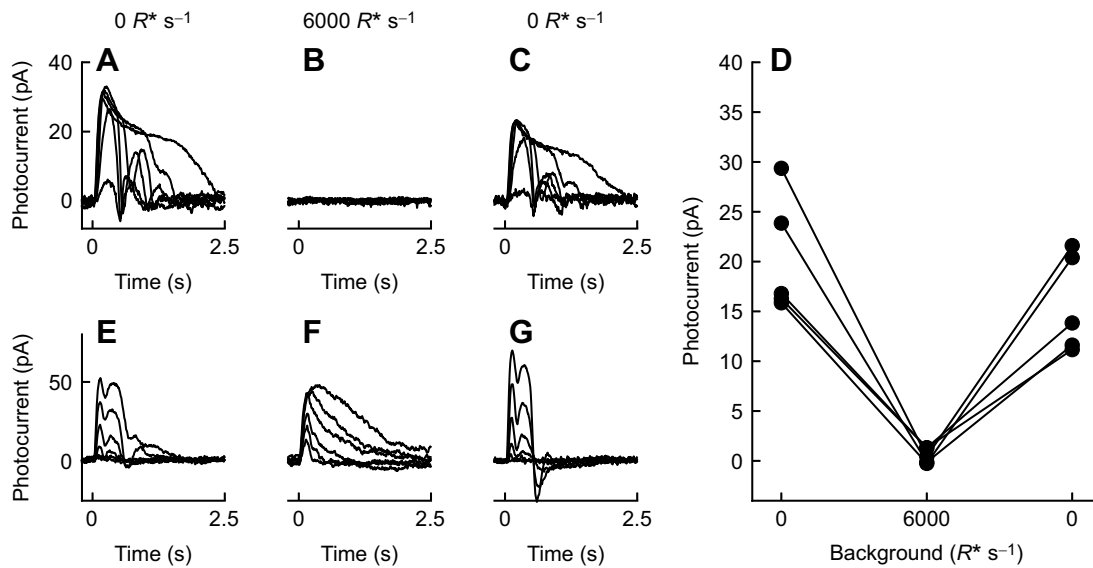


**Fig. 3. Rod OFF bipolar cell light responses are suppressed by background light.** (A) Family of responses to 8 ms, 620 nm flash stimuli of 0.049, 0.33, 1.1, 3.8, 12 and 38  $R^*/rod$ , recorded without a background light. (B) Response family from the same cell as in A but with a 405 nm rod background light of 6000  $R^* s^{-1}$ . Flashes were 6.5, 42, 150, 500, 1500 and 5000  $R^*/rod$ ; or 210, 1400, 4800, 16,000, 48,000 and 160,000  $P^*/cone$ . (C) Response family as in A and B with the same stimuli as in A but after the rod-suppressing background light had been turned off. (D) Maximum light response from 5 OFF bipolar cells like the one in A–C before ( $0 R^* s^{-1}$ ), during ( $6000 R^* s^{-1}$ ) and after ( $0 R^* s^{-1}$ ) the cells were presented with a 405 nm background light of 6000  $R^* s^{-1}$ . The flash stimuli were the same as in A–C. (E) Response family from a dark-adapted, mixed OFF bipolar cell with no background light. Stimuli were 0.0052, 0.034, 0.12, 0.41, 1.23 and 4.1  $R^*/rod$ . (F) Response family as in E but with a 405 nm rod-suppressing background light of 6000  $R^* s^{-1}$ . Stimuli were 6.5, 42, 150, 500, 1500 and 5000  $R^*/rod$ ; or 210, 1400, 4800, 16,000, 48,000 and 160,000  $P^*/cone$ . (G) Response family as in E with the same stimuli but after the rod-suppressing background light had been turned off.

### Lamprey rod bipolar cells

These results show that lamprey have a class of bipolar cell apparently receiving input exclusively from rods, which is OFF unlike the ON rod or rod-dominated bipolar cells in many gnathostome vertebrates. These cells occur in a row in close proximity to the OPL and seem to be fairly abundant. We cannot exclude the possibility that they have a small amount of cone input, which was diminished perhaps as a result of slicing of the retina to prepare the tissue for recording. This input would have been quite small, however, as we never detected any sign of cone input in all 5 cells of Fig. 3D or in the waveform of any of the responses that we recorded from this cell population.

Results from fish (Ashmore and Falk, 1980; Connaughton, 2001; Ishida et al., 1980; Scholes, 1975) and mammals (Shekhar et al., 2016; West and Cepko, 2021) seem to suggest that ON rod bipolar cells with little or no cone input emerged early in evolution and became the dominant pathway for conveying rod signals from the OPL to amacrine and ganglion cells in the IPL. Our results indicate that the processing of rod input in the lamprey retina may be quite different, and that mechanisms of retinal integration may have been more fluid during evolution than previous results have suggested. It seems possible that cells receiving only rod input could be used in making wavelength discriminations in mesopic illumination, when rods and cones are both functioning. Rods are known to be able to participate in wavelength discrimination in mammals, including humans (see Fain and Sampath, 2018). Future experiments may help us understand how the lamprey processes rod and cone signals and provide new insight into the evolution of signal integration in the retina.

### Acknowledgements

We thank Ala Morshedian for help with animals and Jane Hu Coffman and Chunni Zhu for technical assistance.

### Competing interests

The authors declare no competing or financial interests.

### Author contributions

Conceptualization: R.F., G.L.F., A.P.S.; Methodology: R.F., A.P.S.; Validation: R.F.; Investigation: R.F.; Writing - original draft: R.F., G.L.F.; Writing - review & editing: R.F., G.L.F., A.P.S.; Visualization: R.F.; Funding acquisition: G.L.F., A.P.S.

### Funding

This work was supported by a grant from the Great Lakes Fishery Commission, by National Institutes of Health Grants EY001844 (G.L.F.) and EY29817 (A.P.S.), by an unrestricted grant from Research to Prevent Blindness USA to the UCLA Department of Ophthalmology, and by National Eye Institute Core Grant EY00311 to the Stein Eye Institute. Deposited in PMC for release after 12 months.

### Data availability

Data are available on Figshare at: <https://doi.org/10.6084/m9.figshare.19528999>.

### References

- Ashmore, J. F. and Falk, G. (1980). Responses of rod bipolar cells in the dark-adapted retina of the dogfish, *Scyliorhinus canicula*. *J. Physiol.* **300**, 115–150. doi:10.1113/jphysiol.1980.sp013155
- Behrens, C., Schubert, T., Haverkamp, S., Euler, T. and Berens, P. (2016). Connectivity map of bipolar cells and photoreceptors in the mouse retina. *Elife* **5**, e20041. doi:10.7554/eLife.20041.025
- Connaughton, V. P. (2001). Organization of ON- and OFF-pathways in the zebrafish retina: neurotransmitter localization, electrophysiological responses of bipolar cells, and patterns of axon terminal stratification. *Prog. Brain Res.* **131**, 161–176. doi:10.1016/S0079-6123(01)31014-2
- Connaughton, V. P., Graham, D. and Nelson, R. (2004). Identification and morphological classification of horizontal, bipolar, and amacrine cells within the zebrafish retina. *J. Comp. Neurol.* **477**, 371–385. doi:10.1002/cne.20261
- Dacheux, R. F. and Raviola, E. (1986). The rod pathway in the rabbit retina: a depolarizing bipolar and amacrine cell. *J. Neurosci.* **6**, 331–345. doi:10.1523/JNEUROSCI.06-02-00331.1986
- Dickson, D. H. and Graves, D. A. (1979). Fine structure of the lamprey photoreceptors and retinal pigment epithelium (*Petromyzon marinus* L.). *Exp. Eye Res.* **29**, 45–60. doi:10.1016/0014-4835(79)90165-9

- Ellis, E., Frederiksen, R., Morshedian, A., Fain, G. L. and Sampath, A. P. (2020). Separate ON and OFF pathways in vertebrate vision first arose during the Cambrian. *Curr. Biol.* **30**, R633–R634. doi:10.1016/j.cub.2020.04.032
- Fain, G. L. (1975). Interactions of rod and cone signals in the mudpuppy retina. *J. Physiol. (Lond)* **252**, 735–769. doi:10.1113/jphysiol.1975.sp011168
- Fain, G. L. and Sampath, A. P. (2018). Rod and cone interactions in the retina. *F1000Research* **7**, 657. doi:10.12688/f1000research.14412.1
- Govardovskii, V. I., Fyhrquist, N., Reuter, T., Kuzmin, D. G. and Donner, K. (2000). In search of the visual pigment template. *Vis. Neurosci.* **17**, 509–528. doi:10.1017/S0952523800174036
- Grimes, W. N., Baudin, J., Azevedo, A. W. and Rieke, F. (2018). Range, routing and kinetics of rod signaling in primate retina. *Elife* **7**, e38281. doi:10.7554/eLife.38281.027
- Hack, I., Peichl, L. and Brandstätter, J. H. (1999). An alternative pathway for rod signals in the rodent retina: rod photoreceptors, cone bipolar cells, and the localization of glutamate receptors. *Proc. Natl. Acad. Sci. USA* **96**, 14130–14135. doi:10.1073/pnas.96.24.14130
- Hárosi, F. I. and Kleinschmidt, J. (1993). Visual pigments in the sea lamprey, *Petromyzon marinus*. *Vis. Neurosci.* **10**, 711–715. doi:10.1017/S0952523800005411
- Hendrickson, A. (1966). Landolt's club in the amphibian retina: a Golgi and electron microscope study. *Invest. Ophthalmol* **5**, 484–496.
- Hensley, S. H., Yang, X. L. and Wu, S. M. (1993). Relative contribution of rod and cone inputs to bipolar cells and ganglion cells in the tiger salamander retina. *J. Neurophysiol.* **69**, 2086–2098. doi:10.1152/jn.1993.69.6.2086
- Ingram, N. T., Sampath, A. P. and Fain, G. L. (2019). Voltage-clamp recordings of light responses from wild-type and mutant mouse cone photoreceptors. *J. Gen. Physiol.* **151**, 1287–1299. doi:10.1085/jgp.201912419
- Ishida, A. T., Stell, W. K. and Lightfoot, D. O. (1980). Rod and cone inputs to bipolar cells in goldfish retina. *J. Comp. Neurol.* **191**, 315–335. doi:10.1002/cne.901910302
- Kaneko, A. (1970). Physiological and morphological identification of horizontal, bipolar and amacrine cells in goldfish retina. *J. Physiol.* **207**, 623–633. doi:10.1113/jphysiol.1970.sp009084
- Kuraku, S. and Kuratani, S. (2006). Time scale for cyclostome evolution inferred with a phylogenetic diagnosis of hagfish and lamprey cDNA sequences. *Zool. Sci.* **23**, 1053–1064. doi:10.2108/zsj.23.1053
- Li, W., Keung, J. W. and Massey, S. C. (2004). Direct synaptic connections between rods and OFF cone bipolar cells in the rabbit retina. *J. Comp. Neurol.* **474**, 1–12. doi:10.1002/cne.20075
- Morshedian, A. and Fain, G. L. (2017). Light adaptation and the evolution of vertebrate photoreceptors. *J. Physiol.* **595**, 4947–4960. doi:10.1113/JP274211
- Morshedian, A., Toomey, M. B., Pollock, G. E., Frederiksen, R., Enright, J. M., McCormick, S. D., Cornwall, M. C., Fain, G. L. and Corbo, J. C. (2017). Cambrian origin of the CYP27C1-mediated vitamin A1-to-A2 switch, a key mechanism of vertebrate sensory plasticity. *R. Soc. Open Sci.* **4**, 170362. doi:10.1098/rsos.170362
- Okawa, H., Pahlberg, J., Rieke, F., Birnbaumer, L. and Sampath, A. P. (2010). Coordinated control of sensitivity by two splice variants of Galpha(o) in retinal ON bipolar cells. *J. Gen. Physiol.* **136**, 443–454. doi:10.1085/jgp.201010477
- Pang, J.-J., Gao, F., Lem, J., Bramblett, D. E., Paul, D. L. and Wu, S. M. (2010). Direct rod input to cone BCs and direct cone input to rod BCs challenge the traditional view of mammalian BC circuitry. *Proc. Natl. Acad. Sci. USA* **107**, 395–400. doi:10.1073/pnas.0907178107
- Quesada, A. and Génis-Gálvez, J. M. (1985). Morphological and structural study of Landolt's club in the chick retina. *J. Morphol.* **184**, 205–214. doi:10.1002/jmor.1051840210
- Scholes, J. H. (1975). Colour receptors, and their synaptic connexions, in the retina of a cyprinid fish. *Philos. Trans. R. Soc. Lond. B Biol. Sci.* **270**, 61–118. doi:10.1098/rstb.1975.0004
- Shekhar, K., Lapan, S. W., Whitney, I. E., Tran, N. M., Macosko, E. Z., Kowalczyk, M., Adiconis, X., Levin, J. Z., Nemes, J., Goldman, M. et al. (2016). Comprehensive classification of retinal bipolar neurons by single-cell transcriptomics. *Cell* **166**, 1308–1323.e30. doi:10.1016/j.cell.2016.07.054
- Soucy, E., Wang, Y., Nirenberg, S., Nathans, J., Meister, M. (1998). A novel signaling pathway from rod photoreceptors to ganglion cells in mammalian retina. *Neuron* **21**, 481–493. doi:10.1016/S0896-6273(00)80560-7
- Wassle, H., Yamashita, M., Greferath, U., Grunert, U. and Müller, F. (1991). The rod bipolar cell of the mammalian retina. *Vis. Neurosci.* **7**, 99–112. doi:10.1017/S095252380001097X
- Werblin, F. S. and Dowling, J. E. (1969). Organization of the retina of the mudpuppy, *Necturus maculosus*. II. Intracellular recording. *J. Neurophysiol.* **32**, 339–355. doi:10.1152/jn.1969.32.3.339
- West, E. R. and Cepko, C. L. (2021). Development and diversification of bipolar interneurons in the mammalian retina. *Dev. Biol.* **481**, 30–42. doi:10.1016/j.ydbio.2021.09.005
- Wu, S. M., Gao, F. and Maple, B. R. (2000). Functional architecture of synapses in the inner retina: segregation of visual signals by stratification of bipolar cell axon terminals. *J. Neurosci.* **20**, 4462–4470. doi:10.1523/JNEUROSCI.20-12-04462.2000
- Yazulla, S. and Studholme, K. M. (2001). Neurochemical anatomy of the zebrafish retina as determined by immunocytochemistry. *J. Neurocytol.* **30**, 551–592. doi:10.1023/A:1016512617484